



University for the Common Good

Efficiency of internal curing by superabsorbent polymers (SAP) in PC-GGBS mortars

Almeida, Fernando G. ; Klemm, Agnieszka J.

Published in:
Cement and Concrete Composites

DOI:
[10.1016/j.cemconcomp.2018.01.002](https://doi.org/10.1016/j.cemconcomp.2018.01.002)

Publication date:
2018

Document Version
Peer reviewed version

[Link to publication in ResearchOnline](#)

Citation for published version (Harvard):

Almeida, FG & Klemm, AJ 2018, 'Efficiency of internal curing by superabsorbent polymers (SAP) in PC-GGBS mortars', *Cement and Concrete Composites*, vol. 88, pp. 41-51.
<https://doi.org/10.1016/j.cemconcomp.2018.01.002>

General rights

Copyright and moral rights for the publications made accessible in the public portal are retained by the authors and/or other copyright owners and it is a condition of accessing publications that users recognise and abide by the legal requirements associated with these rights.

Take down policy

If you believe that this document breaches copyright please view our takedown policy at <https://edshare.gcu.ac.uk/id/eprint/5179> for details of how to contact us.

Efficiency of internal curing by superabsorbent polymers (SAP) in PC-GGBS mortars

Fernando C.R. Almeida^{1,a} and Agnieszka J. Klemm^{1,b}

¹Glasgow Caledonian University, School of Engineering and Built Environment,
Cowcaddens Road, Glasgow G4 0BA, UK

^afernando.almeida@gcu.ac.uk, ^ba.klemm@gcu.ac.uk

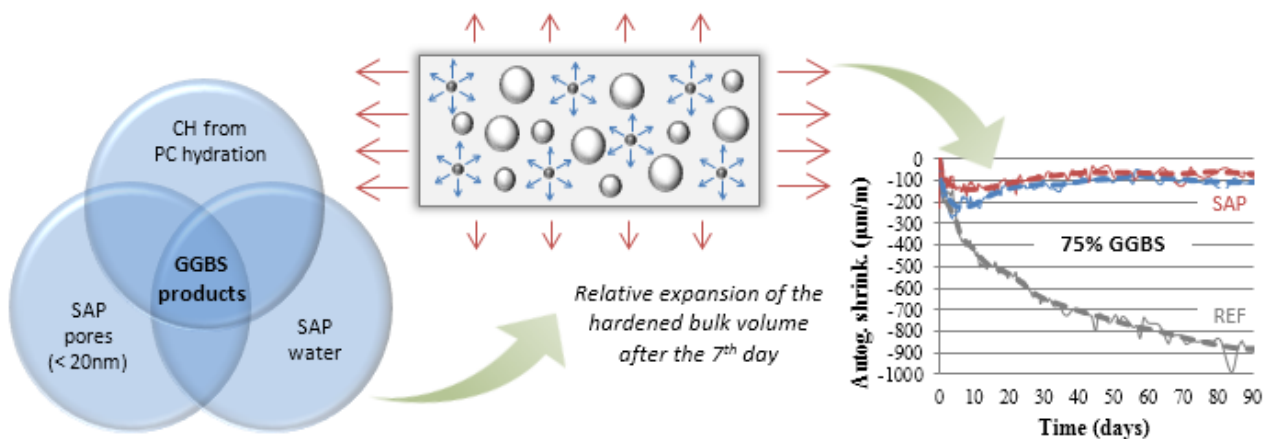
Abstract. This paper evaluates the effect of superabsorbent polymers (SAP) on hydration and microstructure of PC-GGBS mortars. Development of autogenous shrinkage, microstructural characteristics (MIP/SEM) and compressive strength were analysed during the first 90 days. Four levels of Portland cement (PC) replacement by GGBS (0%, 25%, 50% and 75%) and two types of SAP with different water absorption capacities were considered. The results proved the efficiency of internal curing by SAPs in PC-GGBS systems due to significant reduction in autogenous shrinkage, especially for higher contents of GGBS. SAP facilitates GGBS hydration activated by portlandite; its products can be deposited into the nano pores leading to a small relative expansion of the hardened bulk volume. This process is initiated during the second week and it lasts until the sixth week. Despite increased total porosity, compressive strength of SAPs modified mortars is comparable to the reference samples for low GGBS contents in advanced ages.

Keywords: Superabsorbent polymers (SAP), ground granulated blast-furnace slag (GGBS), mortars, autogenous shrinkage, microstructure.

Highlights:

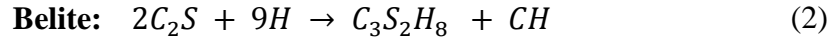
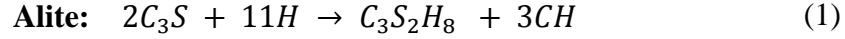
- The higher GGBS content the higher is reduction in autogenous shrinkage by SAPs;
- Precipitation of CSH (from GGBS hydration) is additionally facilitated by the availability of water-filled space provided by collapsed SAPs;
- GGBS hydrated products deposited in pores below 20 nm may lead to a small relative expansion of mortar up to the end of the sixth week;
- SAP does not affect compressive strength for GGBS contents up to 50% and without additional water at 90 days.

Graphical Abstract.

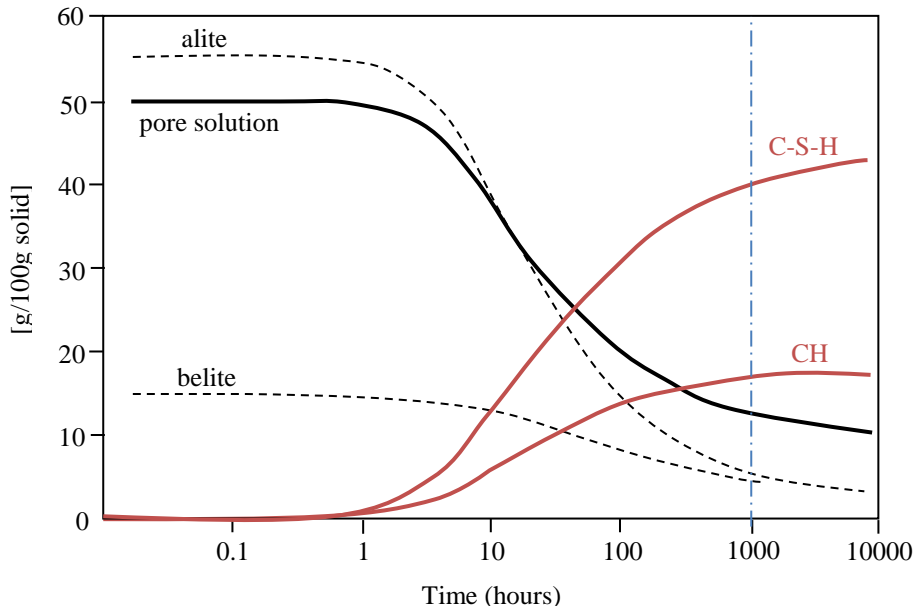


35 **1. Introduction**

36 The main constituents of Portland cement (PC) responsible for gain of strength over time are
37 reactive calcium silicates. Hydration of alite (C_3S) and belite (βC_2S) produce mainly calcium
38 silicate hydrates (CSH) and calcium hydroxide (CH) (Eqs. 1-2).
39



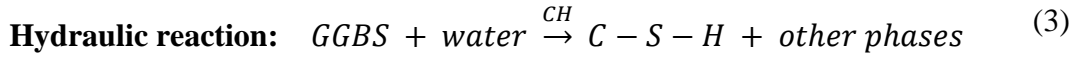
40
41 In cementitious materials, CSH is primarily responsible for its adhesive characteristic, creating a
42 rigid, dense and stable skeleton. Additionally, CH can increase alkalinity and also improve
43 densification of the interfacial transition zone. Thermodynamic modelling shows that more and
44 more CSH and CH are formed with time until a certain level of saturation is reached. For
45 portlandite, it is about 1000h after beginning of hydration (Fig. 1) [1]. Alteration in solid phases
46 during PC hydration implies a decreased pore solution and formation of microstructure which
47 determines hardened properties of concrete.
48



66 **Fig. 1.** Evolution of the main solid phases during the hydration of Portland cement (adapted from [1]).

67
68 However, the rate and extend of reactions can be influenced by the presence of supplementary
69 cementitious materials, such as ground granulated blast-furnace slag (GGBS) [2,3]. GGBS reaction
70 is slower than the reaction of clinker phases, and depends on the chemical composition, fineness,
71 glass content as well as on the composition of interacting solution [3]. The presence of GGBS
72 slightly reduces alkali concentration (due to lower potassium and sodium contents) and pH-values
73 (due to lower OH^- contents) of the blended system. Sulphur species negatively charged, such as
74 sulphide, sulphite and thiosulfate, can additionally decrease OH^- concentration of the pore solution
75 [1,4,5].

76 GGBS presents primarily cementitious behaviour (latent hydraulic activity) but it may also show
77 some minimal pozzolanic features (reaction with CH) [6–8]. Reactivity of GGBS requires,
78 however, an alkaline activator to raise pH in the vicinity of the slag. This is to prevent formation of
79 a thin Si-rich layer on the surface of its grains (during GGBS hydration), which stifles further slag
80 reactions. Thus, PC itself shows as a suitable activator in providing CH and alkali hydroxides
81 [9,10]. Reactivity of slag increases when more PC is present in blended system due to increased pH.
82 Eqs. 3-4 show both GGBS reactions, where CH plays an important role in producing further CSH in
83 a presence of water.



85

86

87

88

89

90

91

92

93

94

95

96

97

98

99

100

101

102

103

104

105

106

107

108

109

110

111

112

113

114

115

116

117

118

119

120

121

122

Nevertheless, there is still no consensus on the mechanisms controlling hydration kinetics especially beyond one day. This is due to the difficulty to quantitatively measure GGBS reaction in blended systems [3]. It is well known that at early ages (up to 30 hours) “filler effects” dominate leading to an increased, and sometimes also faster, reaction of the PC phases. This is due to more space relative to the amount of clinker (dilution effect) and increased nucleation rates [2,3,11–13]. Due to smaller number of clinker grains in a blended system, there is relatively more space for formation of hydrates in early ages and hence the degree of clinker reaction is significantly higher (than in a plain material) [11]. Thus, higher early reaction rate in GGBS systems can reflect on higher chemical shrinkage triggered by self-desiccation process [2,3,14–18]. Additionally, GGBS can refine capillary pores in blended paste and lead to a higher tensile stress generated by the water menisci during hydration processes. Due to the surface tension of water, the force of attraction between pore walls increases as water is consumed, contributing to greater shrinkage [14,18].

However after the first day, there are only speculations that the degree of GGBS reaction could be limited by lack of space filled by early PC hydrated products [2]. Hydration in long term regime is mainly due to C₂S (and perhaps ferrite) phases by the increment of the sheets number in the nanocrystalline regions of CSH [19]. In studies with GGBS matrices, Berodier & Scrivener [20] showed that systems with w/s (water-to-solid) ratios of 0.6 and 0.4 have similar kinetics in the first week, indicating that space does not limit reaction during early ages. Then from the 7th day, reaction slows down in the lower w/s system with less space, while it continues in the higher w/s system. This effect indicates that the slowdown of high content of slag reaction is a result of lack of space in later ages. Thus, there is a minimum critical pore entry radius reached at high degrees of hydration (around 8 nm). Below that, formation of hydrates is restricted by the lack of water-filled capillary pores in later ages. Moreover, reaction of slag could suppress reaction of clinker phases, probably because of a competition for space. According to Scrivener et al [2], although there are no sufficient data on long term hydration to understand the mechanisms operating after 1 day, it is becoming clear that the amount of space available is a critical factor.

Superabsorbent polymers (SAP) have a potential application as internal curing agent for concrete and mortars. Its high capacity to absorb water from fresh mix and release it over time can control autogenous shrinkage in early ages [21–28]. Additionally, when SAP collapses, it leaves behind pores that can significantly change microstructure of hardened concrete and eventually provide more room for later products deposition [29–33].

Although there are some studies related to application of SAP on PC-GGBS materials [34–38] its effects on long term hydration and their microstructure are still unclear and deficient. This paper, therefore, aims to characterize hydration development and evaluate microstructural alterations in mortars with different levels of GGBS content modified by two different types of SAPs. The analysis is carried out by relating results of autogenous shrinkage, MIP/SEM and compressive strength development during 90 days.

123 2. Methodology

124

125

126

127

128

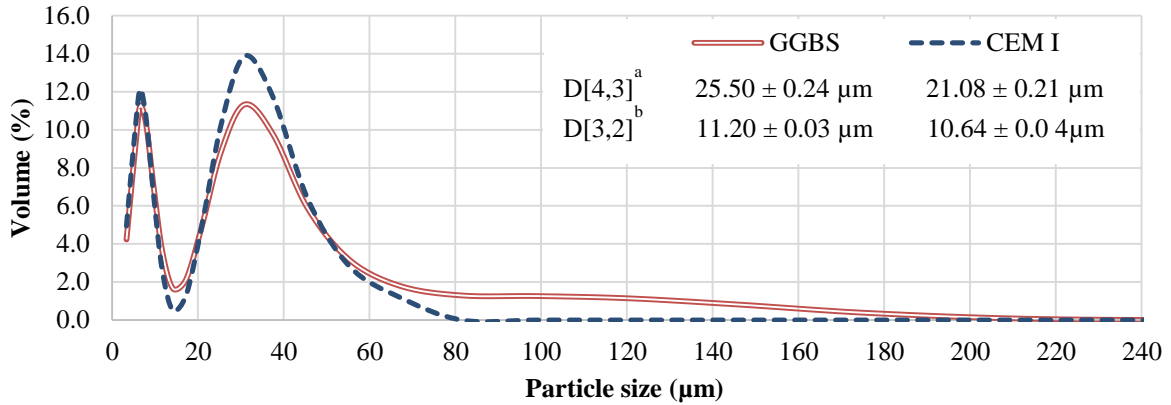
Mortars with different mix proportions have been produced in the experimental programme; four levels of Portland cement (CEM I 52.5N) replacement by GGBS (0%, 25%, 50% and 75%) were adopted. Chemical analysis of CEM I [39] and GGBS [40] are presented in Table 1.

Table 1 – Chemical composition of CEM I and GGBS (%).

	SiO ₂	Al ₂ O ₃	Fe ₂ O ₃	CaO	MgO	SO ₃	Na ₂ O	K ₂ O	LOI
CEM I	20.1	4.9	2.7	62.4	2.2	3.2	0.3	0.6	2.8
GGBS	34.5	13.1	0.2	38.5	9.7	0.4	0.2	0.6	0.6

129
 130
 131
 132
 133
 134
 135
 136
 137
 138
 139
 140
 141
 142
 143
 144
 145
 146
 147
 148
 149
 150
 151
 152
 153
 154
 155
 156
 157
 158
 159
 160
 161

Analysis of particle size distribution by using a Mastersizer laser diffractometer (air as dispersant) showed that GGBS comprises larger particles than CEM I (Fig. 2). While GGBS contained 90% of particles below $49.78 \pm 0.23 \mu\text{m}$, CEM I had the same amount under $41.55 \pm 0.29 \mu\text{m}$. The mean diameters of GGBS and CEM I are shown in Fig. 2; these values were obtained from volume distribution (D[4,3]) and surface area distribution (D[3,2]).



^a D[4,3] = volume mean diameter ^b D[3,2] = surface mean diameter

Fig. 2. Physical characterization of CEM I and GGBS.

Two types of modified polyacrylamide SAPs (provided by BASF Construction Chemicals GmbH, Trostberg, Germany) have been used in the proportion of 0.25% by mass of binder. SAP X and SAP Y had maximum water absorption capacities (WAC) in cement filtrate solution (w/c = 5) of 39 g/g and 47 g/g respectively. They were measured by the tea-bag method up to 3h (max WAC was obtained during the first 30min of testing for both SAPs) [25]. In mixing water, SAP X and SAP Y had WAC of 24 g/g and 32 g/g, respectively. They were measured based on the amount of additional water required to obtain a flow value similar to a reference mortar with w/c ratio of 0.42, i.e., $119 \pm 1 \text{ mm}$ [41–43]. Fig. 3 shows SEM micrographs of both SAPs in dry conditions; they present predominant particles sizes in the range of 30-140 μm and mode values of $95.19 \pm 0.43 \mu\text{m}$ and $85.74 \pm 0.23 \mu\text{m}$ for SAP X and SAP Y, respectively.

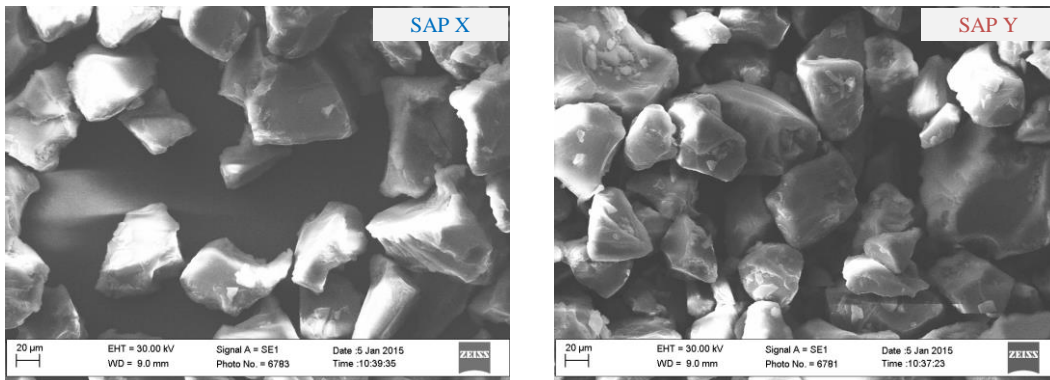


Fig. 3. SEM micrographs of SAP X and SAP Y, respectively.

162
 163
 164
 165
 166
 167
 168
 169

Mortars have been prepared in the proportion of 1:2 (binder: sand) and with water/binder ratio (w/b) of 0.5. This w/b ratio was obtained from the additional amount of water for the SAP with the highest WAC and applied for all mortar samples. Thus, it was assumed that all mortars have an effective w/b ratio greater (or equal to) 0.42, and PC hydration would not be interrupted by lack of water in any time [41,42]. Similar w/b values were used by other authors [33,44]. Fine sand used as fine aggregate contained at least 90% of particles sizes below 0.425 mm [45]. Table 2 shows

170 nomenclature of mortar samples, considering type of SAP and binder content used in this
171 experimental programme.

172
173

Table 2 – Nomenclature of mortars samples.

Sample nomenclature	Type of SAP	CEM I [%]	GGBS [%]
R0		100	0
R25		75	25
R50		50	50
R75		25	75
X0		100	0
X25	SAP X	75	25
X50		50	50
X75		25	75
Y0			100
Y25	SAP Y	75	25
Y50		50	50
Y75		25	75

174

175 Autogenous shrinkage was tested by the sealed corrugated tubes method [46] (average of three
176 specimens for each mortar) from the final setting time to 90 days, using a digital bench dilatometer.
177 In order to identify the autogenous shrinkage tendency, representative and characteristics points
178 were plotted and smoothly connected. Microstructural features and mechanical properties were
179 evaluated after unsealed curing in climate chamber ($T = 21 \pm 2$ °C and $RH = 40 \pm 5\%$) at 7, 14, 28
180 and 90 days. Microstructural characteristics were analysed in terms of total porosity (%) and pore
181 size distribution (nm) using Mercury Intrusion Porosimetry (MIP) technique. Scanning Electron
182 Microscopy (SEM) was used to characterize typical macro pores. Their diameter sizes were
183 measured by Image-J software. Mechanical properties were verified by standard compressive
184 strength determination method from prismatic specimens ($160 \times 40 \times 40$ mm³) [47]; averages of six
185 samples for each mortar were considered.

186 3. Results and discussions

187 3.1 Autogenous shrinkage

188 Fig. 4 shows results of autogenous shrinkage measurements. Overall, SAPs reduced autogenous
189 shrinkage in mortars with and without GGBS compared to the reference samples.

190 Mortars without SAP had the greatest values of autogenous shrinkage, clearly influenced by
191 GGBS level: the greater GGBS content the greater was autogenous shrinkage. For all reference
192 samples, shrinkage sharply increased in the first weeks and reduced its rate from the middle of the
193 second month (considering sealed specimens of corrugated tubes). At 90 days, autogenous
194 shrinkage reached approximate values of -450, -600, -750 and -900 $\mu\text{m}/\text{m}$ for mortars with 0%,
195 25%, 50% and 75% of GGBS respectively.

196 Although relatively high w/b ratio (0.50) has been adopted in this study, significant autogenous
197 shrinkage for the reference mortars was observed. Generally, systems with w/b ratio up to 0.42 are
198 expected to shrink due to self-desiccation processes [41,42]. However, it depends not only on the
199 amount of water but also on the characteristics of cement, especially chemical composition and
200 fineness [48,49]. Autogenous shrinkage greatly depends on the contents and degree of hydration of
201 C_3A and C_4AF . Also, the finer the cement particle, the greater is autogenous shrinkage; the cement
202 fineness induces a finer porous network and hence more intense capillary effects [50,51]. Other
203 studies has found similar autogenous shrinkage values for the reference samples with 0.5 w/b ratio
204 [14,51].

205

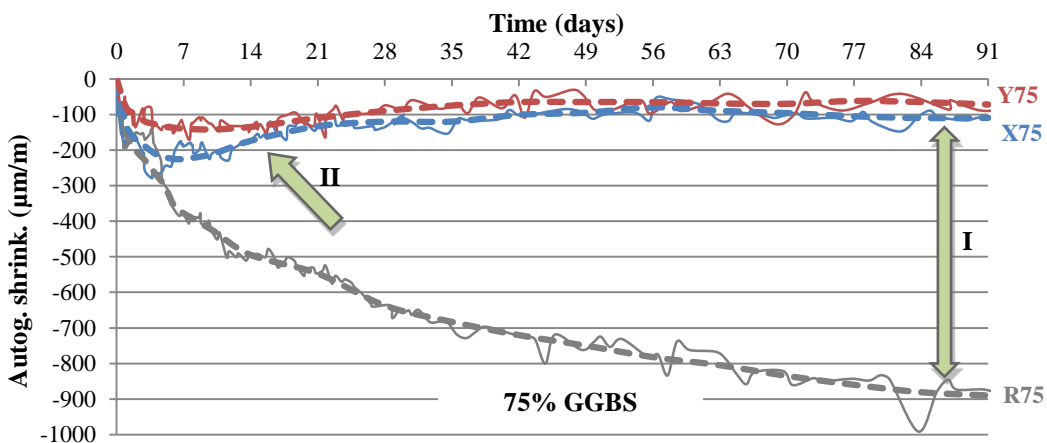
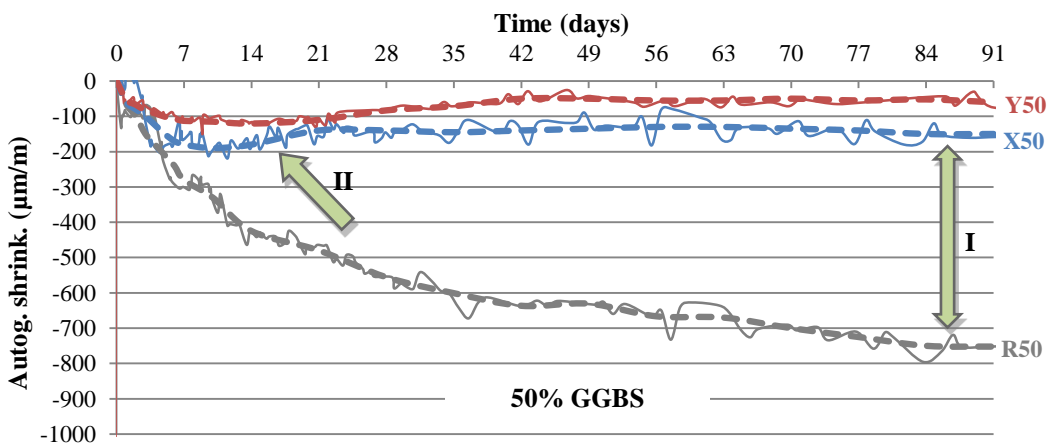
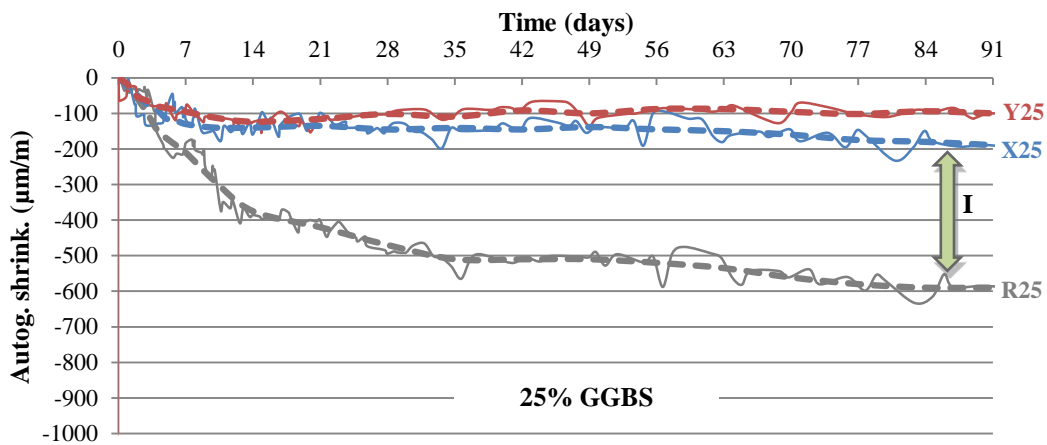
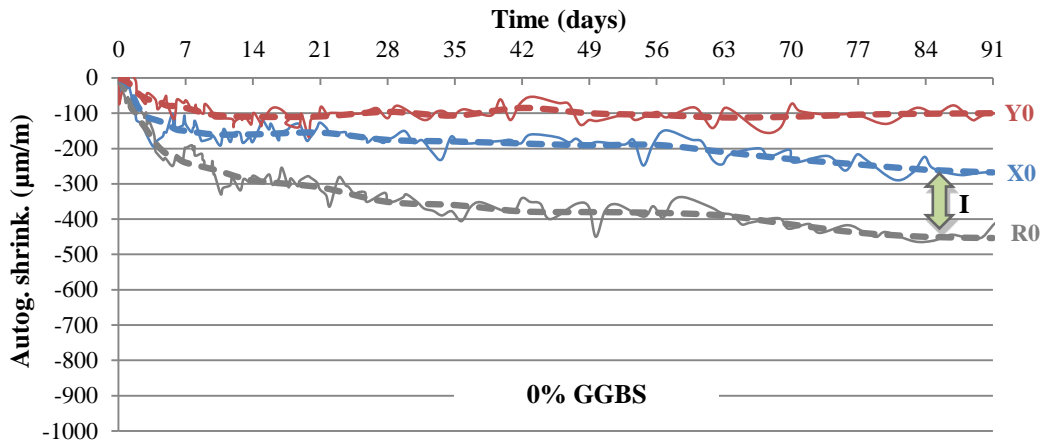


Fig. 4. Autogenous shrinkage development during 90 days (traced lines show autogenous shrinkage tendency). Arrows indicate relevant effects of SAP on PC-GGBS mortars.

206

207

208

209

210

211

212

213 Moreover, when GGBS is added to the mix, autogenous shrinkage is considerably increased. The
214 higher GGBS content the greater is autogenous shrinkage, as reported in the other studies [2,14–
215 18]. This result can be attributed to the physical presence of GGBS, the so-called filler effect. First,
216 the substitution of PC by GGBS at the same w/b ratio indicates a dilution effect. The higher GGBS
217 proportion the lower is the amount of clinker grains. Since GGBS has lower rate of reaction, there is
218 relatively more space for formation of the clinker hydrates at early ages. Therefore, the degree of
219 reaction of clinker component is significantly higher than in GGBS-free material. Additionally,
220 GGBS surfaces may act as nucleation sites for hydrates [2,11]. However, this effect is relatively
221 minor in the present study since PC particles are finer than GGBS ones (Fig. 2). Moreover, addition
222 of GGBS may lead to formation of finer pores, which in turn results in increased autogenous
223 shrinkage. The smaller capillaries the higher is tensile stress triggered by water menisci between
224 pores' walls [14]. Thus, the increment of GGBS content can lead to formation of material, which is
225 more prone to deformation.

226 Addition of SAPs significantly reduced autogenous shrinkage in all mortars when compared to
227 the reference samples. The effectiveness of SAP as an internal curing agent has been proved for
228 plain PC materials [21–27]. SAP Y seemed to be more efficient in reduction of autogenous
229 shrinkage that may be attributed to its higher water absorption capacity. Thus, more water is
230 available in the system that is gradually released. As a result, mortars with SAP Y had the lowest
231 values of shrinkage in comparison with the other samples.

232 Moreover, GGBS level has influenced the behaviour over time and the final performance of
233 mortars with SAP at 90 days. Firstly, the higher GGBS content the more pronounced was reduction
234 in autogenous shrinkage by SAP, as indicated by Arrows I in Fig. 4. Secondly, for low or no GGBS
235 content, mortars with SAP shrank in the first days (although less than the reference samples) and
236 then either stabilized (for SAP Y) or followed in the same pace than the reference sample (for SAP
237 X). However, a slight swelling was noticed in SAP modified mortars with higher GGBS contents
238 (above 50%) after a maximum shrinkage around -200 and -100 $\mu\text{m}/\text{m}$ for SAP X and Y,
239 respectively (Arrows II, Fig. 4). At 75% of GGBS, specimens with both SAPs seem to reach similar
240 values of shrinkage (below -100 $\mu\text{m}/\text{m}$) at later ages. This effect of “relative” expansion (after the
241 maximum shrinkage is reached) seems to be more pronounced for SAP X specimens (with lower
242 water absorption capacity). Other studies have confirmed an expansion in systems when using
243 shrinkage reducing admixtures [35,52].

244 Overall, mortars with SAPs and high GGBS content shrank until the second week and, after that,
245 they started to slightly swell. This effect may be related to the beginning of GGBS hydration
246 facilitated by the presence of SAP as water supplier in certain range of pores (as further discussed).
247 GGBS has reacted with water and the formation of hydrated products led to the “relative”
248 expansion of SAP mortars. When water was consumed and SAP collapsed, no significant external
249 volume changes were noticed, and autogenous shrinkage curves had a tendency to flatten out.

250 Moreover, GGBS reaction is directly related to the saturation of portlandite obtained from PC
251 hydration. According to Fig. 1 [1], most of CH is formed during the first 1000h hydration (or 42
252 days), approximately when mortars with high GGBS contents exhibited maximum relative
253 expansion. The maximum amount of portlandite means the max activation obtained for GGBS
254 hydration, inducing the production of further CSH (Eq. 3). The more CH, the higher is pH in the
255 vicinity of GGBS grains, and hence the higher is the reactivity of slag. These later hydrated
256 products fill extra spaces which were not filled by the cement hydrates due to the lack of clinker
257 [2,53]. CH grains may also contribute to mortar expansion [52], but in a relatively minor manner.
258 This is because in plain PC mortars, no further expansion was observed (Fig. 4). Additionally,
259 although the amount of portlandite in PC-GGBS systems is similar or even higher than in CEM I
260 mortars during the first days (due to this faster clinker reaction caused by filler effect), in long term
261 the amount of CH is generally reduced [3,54,55].

262 On the other hand, no further swelling was observed in mortars without SAP in later ages. It can
263 indicate that there is no sufficient amount of water (present in a specific range of pores, as further
264 discussed) for late reaction of GGBS. In this case, GGBS can act as fine aggregate (finer than fine

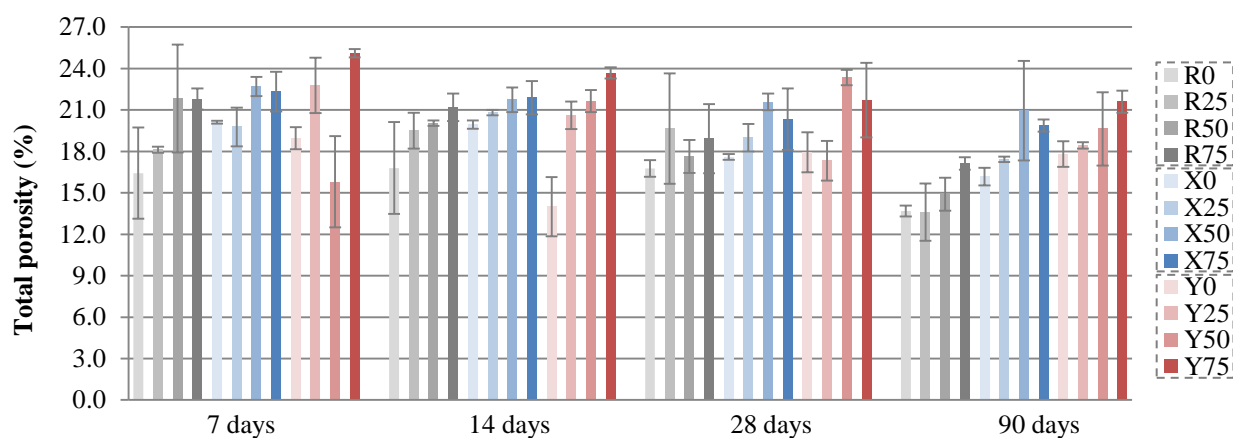
265 sand used) responsible for creation of large amount of finer pores (filler effect). Indeed, its double
 266 role as mineral admixture and very fine aggregate can also be noticed when analysing workability
 267 [36]; GGBS demands more water during mix preparation (for the same consistency) due to its
 268 higher capacity for absorption and adsorption compared with both cement and sand. Consequently,
 269 it increases porosity of mortars when compared to samples without GGBS. Results of
 270 microstructural analysis are discussed in Item 3.2.

271

272 **3.2 Microstructural characteristics**

273 GGBS addition can lead to higher total porosity due to reduction of cement content and decrease
 274 of the total volume of hydrates formed [3]. In general, the higher GGBS content the higher is total
 275 porosity (overall tendency in Fig 5). As the reaction of slag does not lead to such high increases in
 276 solid volume as does the reaction of clinker, total porosity in GGBS systems is expected to be
 277 higher than in plain PC mix [20].

278



279 **Fig. 5.** Results of total porosity by MIP.

280

281
 282 During the first 90 days, a general tendency of increased total porosity by SAP was noted. It was
 283 particularly evident when compared to the reference samples at 90 days. The highest total porosity
 284 values were mainly observed for the polymer with higher WAC; SAP Y was able to absorb more
 285 water from fresh mix and form larger capillary pores when it collapsed. The increment in porosity
 286 by SAP is aligned with other studies [29,44,56–58]. In an ordinary blended system (without SAP),
 287 the degree of GGBS reaction could be limited by the amount of space available to accommodate
 288 hydrated products. It seems that reaction of slag could even suppress the reaction of the clinker
 289 phases due to a competition for space [2,20]. In this context, collapsed SAPs could further help
 290 GGBS products by providing, not only water, but also enough room for later CSH being deposited.

291 Moreover, GGBS addition altered mortars microstructure and changed pore size distribution
 292 patterns. Fig. 6 shows the comparison of pore size distribution curves for samples without and with
 293 75% GGBS at the ages of 7, 14, 28 and 90 days.

294

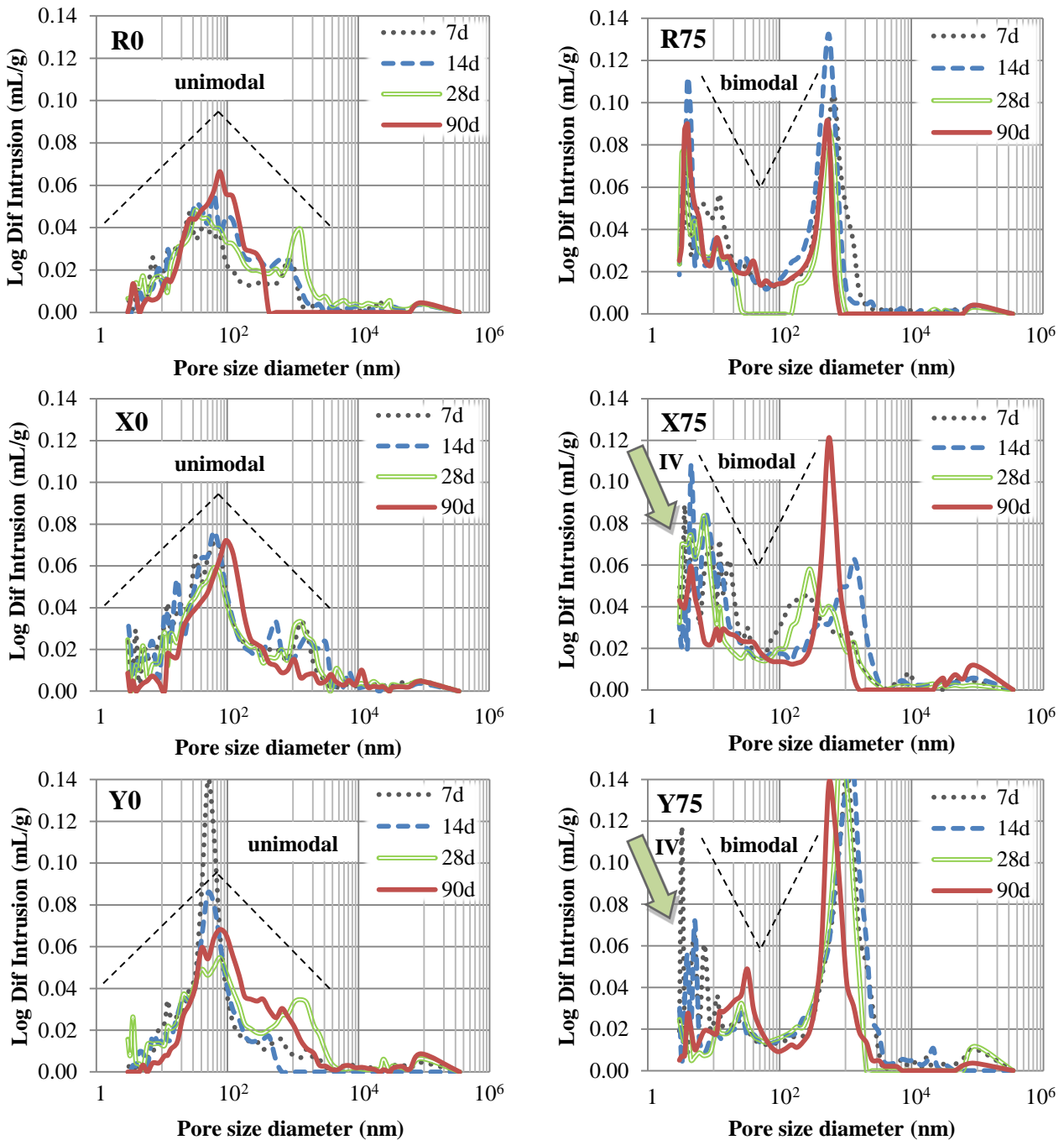


Fig. 6. Unimodal and bimodal distribution for samples with 0% and 75% of GGBS, respectively.

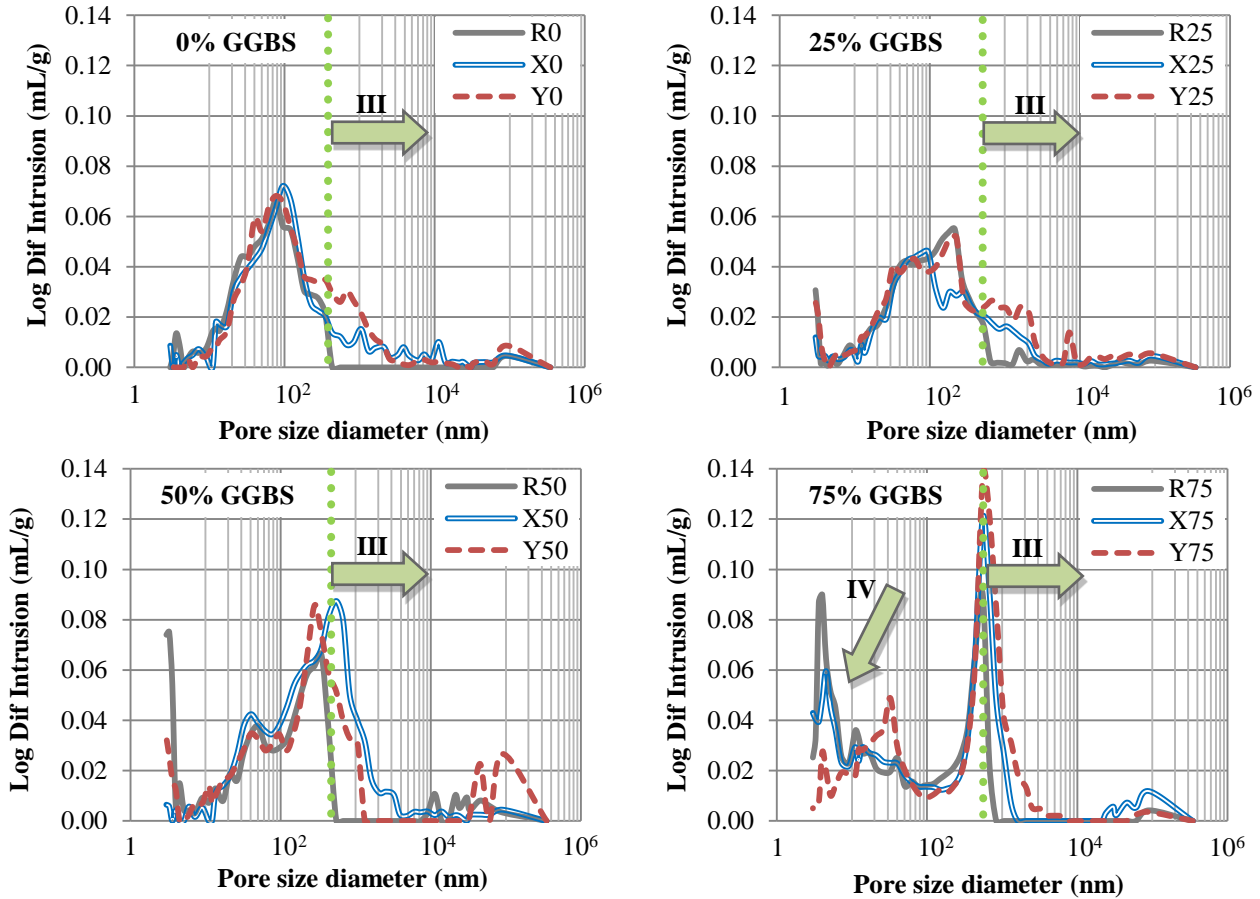
295
296
297
298
299
300
301
302
303
304
305
306
307
308

Pore size distribution curves for mortars with no or lower amount of GGBS are of unimodal shapes, with diameter range between 5-500 nm (peak around 80 nm). However, as GGBS content was increased, bimodal curves started to dominate. In particular for high GGBS content, two predominant bands were formed: one with larger pores (200-700 nm) and the other with smaller pores (below 50 nm). Firstly, the presence of larger particles of GGBS when compared to CEM I (Fig. 2) could form the band with peak around 400 nm. These larger particles could be responsible for reduction of GGBS reactivity and hence for an increase of mortars porosity. Also, GGBS can decrease total volume of hydrates formed in a blended system, increasing its porosity [3]. Secondly, GGBS can produce finer capillaries due to its filler effect [2,14]; its particles are smaller than fine sand. Also, the greater water demand in fresh mix [36] can indicate that GGBS grains absorb/adsorb more water than other dry materials. The availability of more water attached to GGBS particles could promote creation of denser network of CSH, with the predominance of pores under 50 nm of

309 diameter. The results showed that both models (unimodal curves for 0% of GGBS and bimodal
 310 curves for mortars with 75% of GGBS) have the same pattern for all samples studied.

311 This GGBS capacity to produce finer pores can directly contribute to autogenous shrinkage
 312 development (Fig. 4). In smaller capillaries, the force of attraction between pore walls due to water
 313 surface tension is increased. Thus, higher tensile stress in the capillary pores (for mortars with
 314 GGBS) can result in an increased autogenous shrinkage [14].

315 SAPs can also modify pore size distribution in PC-GGBS mortars, as shown in Fig. 7.
 316



317 **Fig. 7.** Pore size distribution curves of mortars at 90 days. Arrows indicate relevant effects of SAP on PC-
 318 GGBS mortars porosity.
 319

320 Overall, SAPs had a tendency to form larger capillary pores when compared to the reference
 321 samples. Arrows III (Fig. 7) indicate that pores with diameter greater than 500 nm may be formed
 322 by collapsing SAPs. In general, mortars with SAP Y created the largest pores; SAP Y absorbs more
 323 water from fresh mix, and consequently leaves behind larger voids in hardened state. This formation
 324 of larger capillaries resulted in higher total porosity of SAP Y specimens at 90 days when compared
 325 to the other samples (Fig. 5).

326 Formation of larger voids by SAPs can also have an impact on the surface roughness as seen on
 327 SEM micrographs (Fig. 8). Macro pores and big concaves can be clearly identified in SAP samples.
 328 The higher total porosity resulting from macro pore formation in SAP containing specimens,
 329 regardless the amount of water in the mix, have been previously reported [33,44,58]. In particular,
 330 Snoeck et al. [44] found that the diameter size of macro pores was in the range of $270 \pm 54 \mu\text{m}$ for
 331 PC mortars using SAPs with similar particle sizes and WAC. These values are in the same order as
 332 those showed in Fig. 8, for typical macro pores in SAP mortars at 90 days.
 333

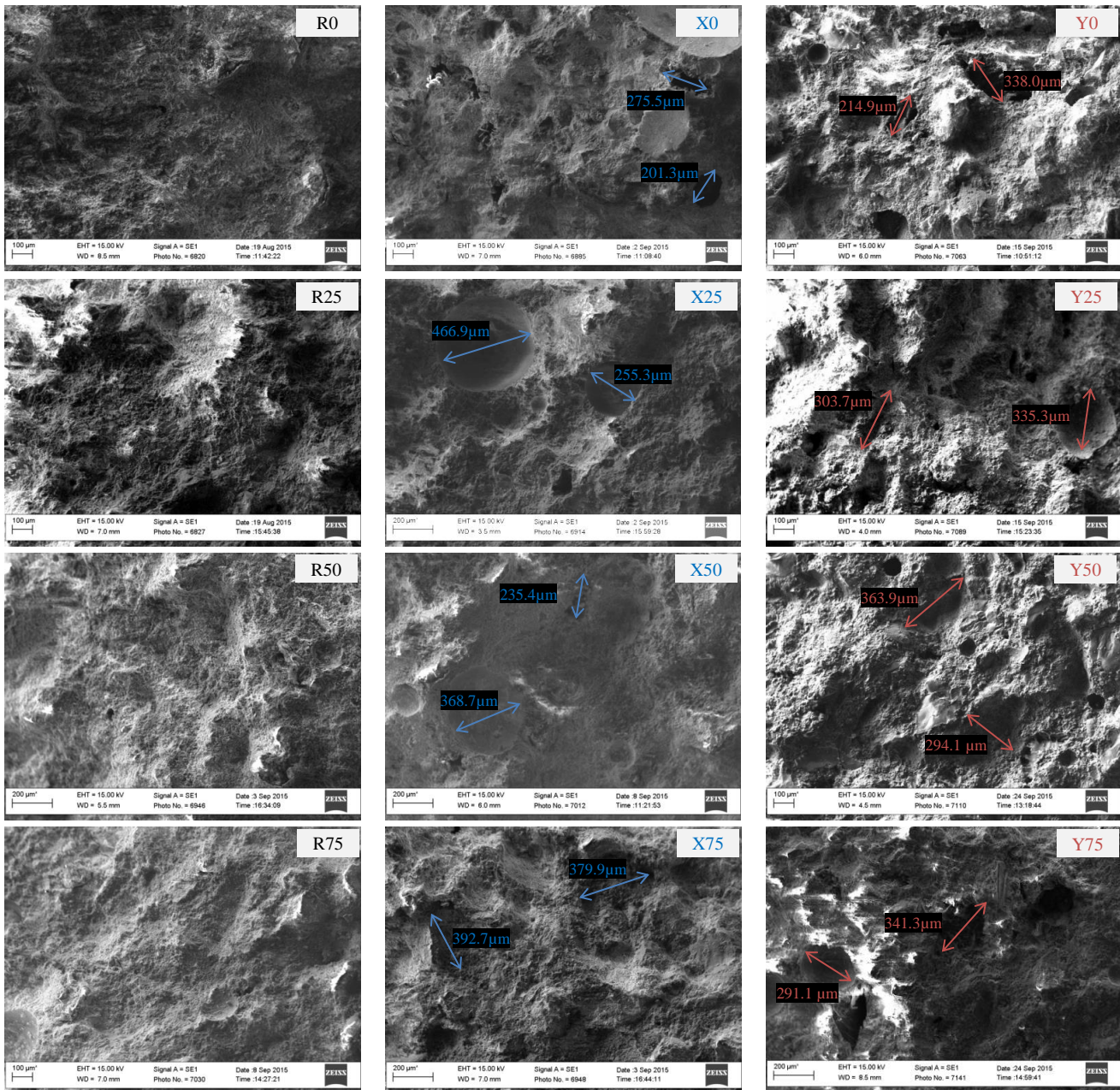


Fig. 8. SEM micrographs of mortars at 90 days. Higher roughness surface can be observed in samples modified by SAPs when compared to the reference samples. Typical macro pores are indicated on SAP samples.

334
335
336
337
338
339
340
341
342
343
344
345
346
347
348
349
350

Besides producing larger pores, SAPs can also have an effect on smaller pores in mortars with high GGBS content; decreased amount of pores with diameter under 20 nm (indicated by Arrow IV, Fig. 6-7). This reduction can be attributed to the filling of pores with later GGBS hydration products that were facilitated by SAP's water supply. Desorption of SAP is mainly controlled by osmotic pressure in early-ages. After that, there is a detachment between SAP and the pore wall (from the cement matrix). Thus, SAP remaining moisture can be released to the paste under humidity gradient (in form of vapour) for continuous curing in later stages [59]. The water stored by polymer tends to move through smaller pores since they provide more surface area for water to adhere to [60]. Indeed, there is a preference of GGBS products in precipitating into smaller pores in non-saturated-water condition [61,62]. In this context, SAP Y is more efficient to provide additional water for hydration and hence the observed reduction of small pores in high GGBS mortars. On the other hand, no significant reduction was recorded for the reference sample since there was not enough water for further GGBS hydration.

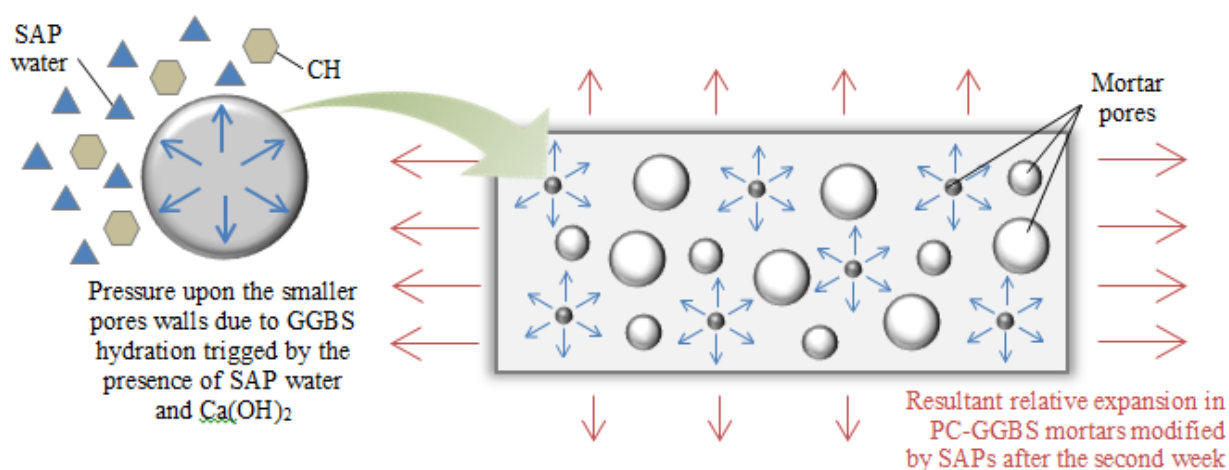
351 As smaller pores are being filled with later hydration products, these products start to exert
352 pressure upon the pore walls. Due to the potential lack of room for CSH precipitation, there is a
353 “space competition” between hydrated products and hardened microstructure. Consequently, this
354 stress leads to the “relative” expansion of the hardened bulk volume in later ages as indicated by
355 Arrows II (Fig. 4).

356 This outcome is in line with findings of Scrivener, Juilland & Monteiro [2]. The authors
357 acknowledge that, despite of the lack of long-term data on GGBS hydration processes, the amount
358 of space available may be a critical factor. Berodier & Scrivener [20] concluded that slag reaction is
359 limited at higher replacement levels due to the lack of space in systems with w/b ratios of 0.6 and
360 0.4. The authors showed that capillary pore space is refined in long term and is soon dominated by
361 pores with sizes approximately between 8-16 nm. These values coincide with those found in the
362 present paper, i.e. pores below 20 nm. Below this diameter range, cementitious reactions (GGBS
363 and clinker phase) are limited by the lack of water-filled capillary pores at later ages. Thus, it seems
364 that there is a space competition for filling the smaller pores with further CSH in long term [2].
365 Therefore, a small relative “expansion” was recorded in SAP-PC-GGBS systems.

366 Indeed, the difference in increased mortar porosity by using different types of SAP has affected
367 autogenous shrinkage development, especially for high GGBS content. Coming back to Fig. 4, it
368 seems that the higher GGBS content the closer is X and Y curves. It can indicate that further
369 external expansion is more pronounced in samples with SAP X. This is because the polymer with
370 lower WAC creates less or smaller pores than SAP Y. Thus, any further formation of hydrated
371 products (due to high content of GGBS) is more likely to provoke relative increase in bulk volume.
372 On the other hand, mortars with SAP Y have higher porosity and hence they can provide more sites
373 for nucleation of late hydration products. These products can also be deposited into the larger SAP
374 Y capillary pores and consequently SAP Y mortars expand less than those with SAP X. In this way,
375 although SAP Y increases porosity (produces larger pores when compared to the other samples), it
376 more efficiently reduces autogenous shrinkage and supply more water and space for further GGBS
377 hydration.

378 Therefore, mechanisms of hardening process in PC-GGBS mortars modified by SAP, during the
379 first 90 days, may be affected by saturation of CH, availability of SAP water and empty spaces for
380 depositing hydrated products. Fig. 9 shows a schematic representation of the effect of nano pores
381 filling on the bulk volume expansion.

382



383

384

385

Fig. 9. GGBS hydration products deposited into smaller pores and its effect on bulk volume expansion.

386

387

388

389

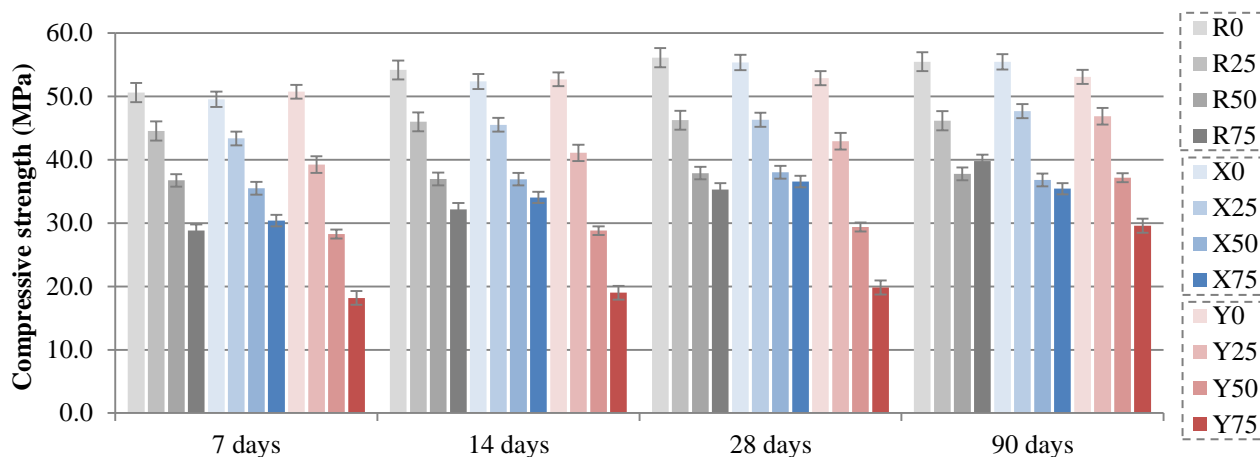
390

Overall, SAP addition increases total porosity in PC-GGBS mortars due to its capacity to create macro pores and larger capillaries in collapsed state. On the other hand, SAP can aid GGBS hydration, contributing to water supply for further reactions in a prolonged time (up to 90 days). The later GGBS reaction is facilitated not only by SAP water (that is adhered to smaller pores, with high surface area) but also by the presence of portlandite from PC hydration (max CH saturation is

391 about 42nd day). Thus, the later hydration products start to form after the second week into the
392 smaller pores (under than 20nm) resulting in an increment of internal compressive stress. This, in
393 turn, leads to a slight “relative” expansion of the bulk volume of SAP mortars with high GGBS
394 contents.

396 3.3 Compressive strength

397 Results of compressive strength are shown in Fig. 10. In general, the higher level of replacement
398 by GGBS the lower compressive strength. This can be related to the higher porosity observed for
399 GGBS mortars due to its lower hydration rate compared to CEM I [3]. It has been shown that 90%
400 of slag has reacted after 3.5 year hydration [5].



414 **Fig. 10.** Results of compressive strength.

417 Mortars with SAP X had a very similar performance to the reference samples. Apart from
418 mortars with high GGBS content at 90 days, all the other samples had compressive strength values
419 in the same order of those without polymer. It can indicate that the increment in porosity by
420 addition of SAP X may not significantly interfere with compressive strength results, especially
421 when lower GGBS levels are considered (up to 50%).

422 Addition of SAP Y to the mix seemed to reduce compressive strength in the first month.
423 However, mortars with this polymer presented comparable results to the reference samples with
424 lower GGBS contents (up to 50%) at 90 days. As SAP X samples, mortars with 75% of GGBS
425 modified by SAP Y also had lower values of strength in comparison to the reference sample. When
426 results were compared over the time, a considerable gain of strength can be noticed for samples
427 with higher GGBS contents and the polymer with higher WAC (samples Y50 and Y75). Although
428 SAP Y has reduced compressive strength because of increased porosity (compared to the reference),
429 it improved the rate of GGBS hydration in later ages. It seemed that GGBS hydrated products may
430 have filled pores formed by SAP Y and significantly increased compressive strength values at 90
431 days (compared to 28 days).

432 Overall, it seemed that SAP may not have significant effect on mechanical properties in
433 advanced ages for lower GGBS contents, even with increased porosity in a unimodal pore size
434 distribution. As GGBS level is increased and its pore size distribution is changed to bimodal curves,
435 the increase in porosity by both SAP and GGBS can be evinced by reduction in strength level. In
436 order to keep the same compressive strength values for mortars with and without SAP, the limit
437 level of PC replacement by GGBS should be 50%. Above this content, decrease in compressive
438 strength takes place.

439
440
441

442 4. Conclusions

443 From the experimental results, the following can be concluded:

- 444 • Mortars with SAP can significantly reduce autogenous shrinkage, especially with higher
445 GGBS contents. After max shrinkage (up to $-200 \mu\text{m/m}$) in the first weeks, mortars with
446 high GGBS level modified by SAPs slightly swell due to the filling of nano pores with later
447 hydration slag products. Further CSH is formed due to the availability of water supplied by
448 SAP and a presence of space created by collapsed SAPs. Also, GGBS reaction is activated
449 by CH formed in PC hydration; the max relative expansion takes place at the end of week 6,
450 when the max amount of portlandite is formed;
- 451 • Both studied SAPs are able to supply water for longer GGBS hydration. Its products can be
452 deposited into the smaller pores (under 20 nm of diameter) formed by high contents of
453 GGBS. It is because smaller pores have greater water affinity due to their higher surface
454 area. SAP Y is more efficient in decreasing the number of smaller pores due to its higher
455 capacity to absorb and also to provide water for later hydration;
- 456 • Pores with diameter greater than 500 nm may be formed by addition of polymer. SAP Y,
457 with higher water absorption capacity, is able to produce larger pores than SAP X. However,
458 this increment of porosity by SAP does not affect compressive strength for low GGBS
459 contents at 90 days (considering the same w/b ratio). Reduction in mechanical properties can
460 be observed for substitution levels above 50% when compared to the reference samples;
- 461 • Overall, although SAP increases total porosity in PC-GGBS mortars, it reduces autogenous
462 shrinkage, extends GGBS hydration, and keeps the same level of compressive strength (for
463 low GGBS contents) when compared to the reference samples with the same w/b ratios.

464 Acknowledgements

465 The authors acknowledge National Council for Scientific and Technological Development
466 (CNPq – Brazil) for the financial support, Hanson Cements for CEM I and GGBS supply, and
467 BASF for SAPs supply.

468 References

- 469 [1] B. Lothenbach, F. Winnefeld, Thermodynamic modelling of the hydration of Portland
470 cement, *Cem. Concr. Res.* 36 (2006) 209–226. doi:10.1016/j.cemconres.2005.03.001.
- 471 [2] K.L. Scrivener, P. Juilland, P.J.M. Monteiro, Advances in understanding hydration of
472 Portland cement, *Cem. Concr. Res.* 78 (2015) 38–56. doi:10.1016/j.cemconres.2015.05.025.
- 473 [3] B. Lothenbach, K. Scrivener, R.D. Hooton, Supplementary cementitious materials, *Cem.*
474 *Concr. Res.* 41 (2011) 1244–1256. doi:10.1016/j.cemconres.2010.12.001.
- 475 [4] A. Vollpracht, B. Lothenbach, R. Snellings, J. Haufe, The pore solution of blended cements:
476 a review, *Mater. Struct.* 49 (2016) 3341–3367. doi:10.1617/s11527-015-0724-1.
- 477 [5] B. Lothenbach, G. Le Saout, M. Ben Haha, R. Figi, E. Wieland, Hydration of a low-alkali
478 CEM III/B–SiO₂ cement (LAC), *Cem. Concr. Res.* 42 (2012) 410–423.
479 doi:10.1016/j.cemconres.2011.11.008.
- 480 [6] S. Kumar, R. Kumar, A. Bandopadhyay, T.C. Alex, B. Ravi Kumar, S.K. Das, S.P. Mehrotra,
481 Mechanical activation of granulated blast furnace slag and its effect on the properties and
482 structure of portland slag cement, *Cem. Concr. Compos.* 30 (2008) 679–685.
483 doi:10.1016/j.cemconcomp.2008.05.005.
- 484 [7] O. Peyronnard, M. Benzaazoua, Estimation of the cementitious properties of various
485 industrial by-products for applications requiring low mechanical strength, *Resour. Conserv.*
486 *Recycl.* 56 (2011) 22–33. doi:10.1016/j.resconrec.2011.08.008.

- 487 [8] A. Oner, S. Akyuz, An experimental study on optimum usage of GGBS for the compressive
488 strength of concrete, *Cem. Concr. Compos.* 29 (2007) 505–514.
489 doi:10.1016/j.cemconcomp.2007.01.001.
- 490 [9] M. Thomas, The effect of supplementary cementing materials on alkali-silica reaction: A
491 review, *Cem. Concr. Res.* 41 (2011) 1224–1231. doi:10.1016/j.cemconres.2010.11.003.
- 492 [10] J.L. Provis, Geopolymers and other alkali activated materials: why, how, and what?, *Mater.*
493 *Struct.* 47 (2014) 11–25. doi:10.1617/s11527-013-0211-5.
- 494 [11] K.L. Scrivener, B. Lothenbach, N. De Belie, E. Gruyaert, J. Skibsted, R. Snellings, A.
495 Vollpracht, TC 238-SCM: hydration and microstructure of concrete with SCMs, *Mater.*
496 *Struct.* 48 (2015) 835–862. doi:10.1617/s11527-015-0527-4.
- 497 [12] G.C. Cordeiro, R.D. Toledo Filho, L.M. Tavares, E.M.R. Fairbairn, Pozzolanic activity and
498 filler effect of sugar cane bagasse ash in Portland cement and lime mortars, *Cem. Concr.*
499 *Compos.* 30 (2008) 410–418. doi:10.1016/j.cemconcomp.2008.01.001.
- 500 [13] F.C.R. Almeida, A. Sales, J.P. Moretti, P.C.D. Mendes, Sugarcane bagasse ash sand (SBAS):
501 Brazilian agroindustrial by-product for use in mortar, *Constr. Build. Mater.* 82 (2015) 31–38.
502 doi:10.1016/j.conbuildmat.2015.02.039.
- 503 [14] M. Valcuende, F. Benito, C. Parra, I. Miñano, Shrinkage of self-compacting concrete made
504 with blast furnace slag as fine aggregate, *Constr. Build. Mater.* 76 (2015) 1–9.
505 doi:10.1016/j.conbuildmat.2014.11.029.
- 506 [15] W. Zhang, Y. Hama, S.H. Na, Drying shrinkage and microstructure characteristics of mortar
507 incorporating ground granulated blast furnace slag and shrinkage reducing admixture, *Constr.*
508 *Build. Mater.* 93 (2015) 267–277. doi:10.1016/j.conbuildmat.2015.05.103.
- 509 [16] C. Jiang, Y. Yang, Y. Wang, Y. Zhou, C. Ma, Autogenous shrinkage of high performance
510 concrete containing mineral admixtures under different curing temperatures, *Constr. Build.*
511 *Mater.* 61 (2014) 260–269. doi:10.1016/j.conbuildmat.2014.03.023.
- 512 [17] M. Bouasker, N.E.H. Khalifa, P. Mounanga, N. Ben Kahla, Early-age deformation and
513 autogenous cracking risk of slag–limestone filler-cement blended binders, *Constr. Build.*
514 *Mater.* 55 (2014) 158–167. doi:10.1016/j.conbuildmat.2014.01.037.
- 515 [18] K.M. Lee, H.K. Lee, S.H. Lee, G.Y. Kim, Autogenous shrinkage of concrete containing
516 granulated blast-furnace slag, *Cem. Concr. Res.* 36 (2006) 1279–1285.
517 doi:10.1016/j.cemconres.2006.01.005.
- 518 [19] A.C.A. Muller, K.L. Scrivener, A.M. Gajewicz, P.J. McDonald, Densification of C–S–H
519 Measured by ¹H NMR Relaxometry, *J. Phys. Chem. C.* 117 (2013) 403–412.
520 doi:10.1021/jp3102964.
- 521 [20] E. Berodier, K. Scrivener, Evolution of pore structure in blended systems, *Cem. Concr. Res.*
522 73 (2015) 25–35. doi:10.1016/j.cemconres.2015.02.025.
- 523 [21] V. Mechtcherine, H.-W. Reinhardt, eds., Application of Superabsorbent Polymers (SAP) in
524 Concrete Construction: State-of-the-Art Report Prepared by Technical Committee 225-SAP,
525 Springer, RILEM, 2012. doi:10.1007/978-94-007-2733-5.
- 526 [22] V. Mechtcherine, M. Gorges, C. Schroefl, A. Assmann, W. Brameshuber, A.B. Ribeiro, D.
527 Cusson, J. Custódio, E.F. Silva, K. Ichimiya, S. Igarashi, A. Klemm, K. Kovler, A.N.
528 Mendonça Lopes, P. Lura, V.T. Nguyen, H.-W. Reinhardt, R.D.T. Filho, J. Weiss, M.
529 Wyrzykowski, G. Ye, S. Zhutovsky, Effect of internal curing by using superabsorbent
530 polymers (SAP) on autogenous shrinkage and other properties of a high-performance fine-
531 grained concrete: results of a RILEM round-robin test, *Mater. Struct.* 47 (2013) 541–562.
532 doi:10.1617/s11527-013-0078-5.

- 533 [23] B. Craeye, M. Geirnaert, G. De Schutter, Super absorbing polymers as an internal curing
534 agent for mitigation of early-age cracking of high-performance concrete bridge decks,
535 *Constr. Build. Mater.* 25 (2011) 1–13. doi:10.1016/j.conbuildmat.2010.06.063.
- 536 [24] M.T. Hasholt, O.M. Jensen, K. Kovler, S. Zhutovsky, Can superabsorbent polymers mitigate
537 autogenous shrinkage of internally cured concrete without compromising the strength?,
538 *Constr. Build. Mater.* 31 (2012) 226–230. doi:10.1016/j.conbuildmat.2011.12.062.
- 539 [25] C. Schröfl, V. Mechtcherine, M. Gorges, Relation between the molecular structure and the
540 efficiency of superabsorbent polymers (SAP) as concrete admixture to mitigate autogenous
541 shrinkage, *Cem. Concr. Res.* 42 (2012) 865–873. doi:10.1016/j.cemconres.2012.03.011.
- 542 [26] D. Shen, X. Wang, D. Cheng, J. Zhang, G. Jiang, Effect of internal curing with super
543 absorbent polymers on autogenous shrinkage of concrete at early age, *Constr. Build. Mater.*
544 106 (2016) 512–522. doi:10.1016/j.conbuildmat.2015.12.115.
- 545 [27] A.J. Klemm, F.C.R. Almeida, Application of Superabsorbent polymers as novel admixture
546 for cementitious materials, *Concr. Plant Int. J.* (2016) 38–46.
- 547 [28] A.N.M. Lopes, E.F. Silva, D.C.C. Dal Molin, R.D. Toledo Filho, Shrinkage-reducing
548 admixture: Effects on durability of high-strength concrete, *ACI Mater. J.* 110 (2013) 365–
549 374.
- 550 [29] A.J. Klemm, K.S. Sikora, The effect of Superabsorbent Polymers (SAP) on microstructure
551 and mechanical properties of fly ash cementitious mortars, *Constr. Build. Mater.* 49 (2013)
552 134–143. doi:10.1016/j.conbuildmat.2013.07.039.
- 553 [30] H. Gonçalves, B. Gonçalves, L. Silva, N. Vieira, F. Raupp-Pereira, L. Senff, J.A. Labrincha,
554 The influence of porogene additives on the properties of mortars used to control the ambient
555 moisture, *Energy Build.* 74 (2014) 61–68. doi:10.1016/j.enbuild.2014.01.016.
- 556 [31] D. Snoeck, L.F. Velasco, A. Mignon, S. Van Vlierberghe, P. Dubruel, P. Lodewyckx, N. De
557 Belie, The effects of superabsorbent polymers on the microstructure of cementitious
558 materials studied by means of sorption experiments, *Cem. Concr. Res.* 77 (2015) 26–35.
559 doi:10.1016/j.cemconres.2015.06.013.
- 560 [32] M.T. Hasholt, O.M. Jensen, Chloride migration in concrete with superabsorbent polymers,
561 *Cem. Concr. Compos.* 55 (2015) 290–297. doi:10.1016/j.cemconcomp.2014.09.023.
- 562 [33] V. Mechtcherine, C. Schroefl, M. Wyrzykowski, M. Gorges, P. Lura, D. Cusson, J.
563 Margeson, N. De Belie, D. Snoeck, K. Ichimiya, V. Falikman, S. Friedrich, Effect of
564 superabsorbent polymers (SAP) on the freeze – thaw resistance of concrete : results of a
565 RILEM interlaboratory study, *Mater. Struct.* 50 (2017). doi:10.1617/s11527-016-0868-7.
- 566 [34] H. Beushausen, M. Gillmer, M. Alexander, The influence of superabsorbent polymers on
567 strength and durability properties of blended cement mortars, *Cem. Concr. Compos.* 52
568 (2014) 73–80. doi:10.1016/j.cemconcomp.2014.03.008.
- 569 [35] D. Snoeck, O.M. Jensen, N. De Belie, The influence of superabsorbent polymers on the
570 autogenous shrinkage properties of cement pastes with supplementary cementitious
571 materials, *Cem. Concr. Res.* 74 (2015) 59–67. doi:10.1016/j.cemconres.2015.03.020.
- 572 [36] F. do Couto Rosa Almeida, A.J. Klemm, Effect of Superabsorbent Polymers (SAP) on Fresh
573 State Mortars with Ground Granulated Blast-Furnace Slag (GGBS), in: 5th Int. Conf. Durab.
574 *Concr. Struct.*, Shenzhen, 2016. doi:10.5703/1288284316136.
- 575 [37] C. Song, Y.C. Choi, S. Choi, Effect of internal curing by superabsorbent polymers – Internal
576 relative humidity and autogenous shrinkage of alkali-activated slag mortars, *Constr. Build.*
577 *Mater.* 123 (2016) 198–206. doi:10.1016/j.conbuildmat.2016.07.007.
- 578 [38] M. Wyrzykowski, P. Lura, Reduction of Autogenous Shrinkage in Opc and Bfsc, in: XIII Int.

- 579 Conf. Durab. Build. Mater. Components - XIII DBMC, Sao Paulo, 2015: pp. 999–1005.
- 580 [39] BS-EN 197-1, Cement Part 1: Composition, Specifications and Conformity Criteria for
581 Common Cements (2011).
- 582 [40] BS EN 15167-1, Ground granulated blast furnace slag for use in concrete , mortar and grout -
583 Part 1: Definitions, specifications and conformity criteria (2006).
- 584 [41] T. Powers, Absorption of Water by Portland Cement Paste during the Hardening Process,
585 Ind. Eng. Chem. 27 (1935) 790–794. doi:10.1021/ie50307a011.
- 586 [42] O.M. Jensen, P.F. Hansen, Water-entrained cement-based materials: I. Principles and
587 theoretical background, Cem. Concr. Res. 32 (2001) 973–978. doi:10.1016/S0008-
588 8846(01)00463-X.
- 589 [43] EN 1015-3, Methods of Test for Mortar for Masonry - Part 3: Determination of consistence
590 of fresh mortar (by flow table) (2006).
- 591 [44] D. Snoeck, D. Schaubroeck, P. Dubruel, N. De Belie, Effect of high amounts of
592 superabsorbent polymers and additional water on the workability, microstructure and
593 strength of mortars with a water-to-cement ratio of 0.50, Constr. Build. Mater. 72 (2014)
594 148–157. doi:10.1016/j.conbuildmat.2014.09.012.
- 595 [45] BS EN 13139, Aggregates for mortar (2013).
- 596 [46] ASTM-C1698-09, Standard Test Method for Autogenous Strain of Cement Paste and
597 Mortars (2009).
- 598 [47] BS EN 1015-11, Methods of Test for Mortar for Masonry - Part 11: Determination of
599 Flexural and Compressive Strength of Hardened Mortar (2006).
- 600 [48] A. Alrifai, S. Aggoun, E.-H. Kadri, G. De Schutter, A. Noumowe, Influence of aggregate
601 skeleton on shrinkage properties: validation of the model developed by Le Roy for the case
602 of self-compacting concrete, Mater. Struct. 44 (2011) 1593–1607. doi:10.1617/s11527-011-
603 9721-1.
- 604 [49] E. Tazawa, S. Miyazawa, Influence of cement and admixture on autogenous shrinkage of
605 cement paste, Cem. Concr. Res. 25 (1995) 281–287. doi:10.1016/0008-8846(95)00010-0.
- 606 [50] P. Mounanga, M. Bouasker, A. Pertue, A. Perronnet, A. Khelidj, Early-age autogenous
607 cracking of cementitious matrices: physico-chemical analysis and micro/macro
608 investigations, Mater. Struct. 44 (2011) 749–772. doi:10.1617/s11527-010-9663-z.
- 609 [51] Z. Jiang, Z. Sun, P. Wang, Autogenous relative humidity change and autogenous shrinkage
610 of high-performance cement pastes, Cem. Concr. Res. 35 (2005) 1539–1545.
611 doi:10.1016/j.cemconres.2004.06.028.
- 612 [52] G. Sant, B. Lothenbach, P. Juilland, G. Le Saout, J. Weiss, K. Scrivener, The origin of early
613 age expansions induced in cementitious materials containing shrinkage reducing admixtures,
614 Cem. Concr. Res. 41 (2011) 218–229. doi:10.1016/j.cemconres.2010.12.004.
- 615 [53] A. Pourjavadi, S.M. Fakoopoor, P. Hosseini, A. Khaloo, Interactions between
616 superabsorbent polymers and cement-based composites incorporating colloidal silica
617 nanoparticles, Cem. Concr. Compos. 37 (2013) 196–204.
618 doi:10.1016/j.cemconcomp.2012.10.005.
- 619 [54] I. Pane, W. Hansen, Investigation of blended cement hydration by isothermal calorimetry and
620 thermal analysis, Cem. Concr. Res. 35 (2005) 1155–1164.
621 doi:10.1016/j.cemconres.2004.10.027.
- 622 [55] J. Escalante, L.. Gómez, K. Johal, G. Mendoza, H. Mancha, J. Méndez, Reactivity of blast-
623 furnace slag in Portland cement blends hydrated under different conditions, Cem. Concr. Res.

- 624 31 (2001) 1403–1409. doi:10.1016/S0008-8846(01)00587-7.
- 625 [56] J. Justs, M. Wyrzykowski, D. Bajare, P. Lura, Internal curing by superabsorbent polymers in
626 ultra-high performance concrete, *Cem. Concr. Res.* 76 (2015) 82–90.
627 doi:10.1016/j.cemconres.2015.05.005.
- 628 [57] O.M. Jensen, P.F. Hansen, Water-entrained cement-based materials: II. Experimental
629 observations, *Cem. Concr. Res.* 32 (2002) 973–978. doi:10.1016/S0008-8846(02)00737-8.
- 630 [58] S. Laustsen, M.T. Hasholt, O.M. Jensen, Void structure of concrete with superabsorbent
631 polymers and its relation to frost resistance of concrete, *Mater. Struct.* 48 (2015) 357–368.
632 doi:10.1617/s11527-013-0188-0.
- 633 [59] F. Wang, J. Yang, S. Hu, X. Li, H. Cheng, Influence of superabsorbent polymers on the
634 surrounding cement paste, *Cem. Concr. Res.* 81 (2016) 112–121.
635 doi:10.1016/j.cemconres.2015.12.004.
- 636 [60] D.E. Ramos, Walnut Production Manual, University of California, Division of Agriculture
637 and Natural Resources, Communication Services-Publications, 1998.
- 638 [61] K. Li, Q. Zeng, M. Luo, X. Pang, Effect of self-desiccation on the pore structure of paste and
639 mortar incorporating 70% GGBS, *Constr. Build. Mater.* 51 (2014) 329–337.
640 doi:10.1016/j.conbuildmat.2013.10.063.
- 641 [62] Y.C. Choi, J. Kim, S. Choi, Mercury intrusion porosimetry characterization of micropore
642 structures of high-strength cement pastes incorporating high volume ground granulated blast-
643 furnace slag, *Constr. Build. Mater.* 137 (2017) 96–103.
644 doi:10.1016/j.conbuildmat.2017.01.076.
- 645
- 646